MDGA1 negatively regulates amyloid precursor protein–mediated synapse inhibition in the hippocampus

Jinhu Kim[a,1], Seungjoon Kim[a,1], Hyeonho Kim[a,2], In-Wook Hwang[b,2], Sungwon Bae[a], Sudeep Karki[c], Dongwook Kim[a], Roberto Ogelman[b], Geul Bang[d], Jin Young Kim[d], Tommi Kajander[c], Ji Won Um[a], Won Chan Oh[b,3], and Jaewon Ko[a,3]

[a]Department of Brain and Cognitive Sciences, Daegu Gyeongbuk Institute of Science and Technology, Daegu 42988, Korea; [b]Department of Pharmacology, University of Colorado School of Medicine, Aurora, CO 80045; [c]Institute of Biotechnology, University of Helsinki, 00014 Helsinki, Finland; and [d]Research Center for Bioconvergence Analysis, Korea Basic Science Institute, Ochang 305-732, Korea

Edited by Hee-Sup Shin, Center for Cognition and Sociality, Institute for Basic Science, Daejeon, South Korea; received August 19, 2021; accepted December 5, 2021

Balanced synaptic inhibition, controlled by multiple synaptic adhesion proteins, is critical for proper brain function. MDGA1 (meprin, A-5 protein, and receptor protein-tyrosine phosphatase mu [MAM] domain-containing glycosylphosphatidylinositol anchor protein 1) suppresses synaptic inhibition in mammalian neurons, yet the molecular mechanisms underlying MDGA1-mediated negative regulation of GABAergic synapses remain unresolved. Here, we show that the MDGA1 MAM domain directly interacts with the extension domain of amyloid precursor protein (APP). Strikingly, MDGA1-mediated synaptic disinhibition requires the MDGA1 MAM domain and is prominent at distal dendrites of hippocampal CA1 pyramidal neurons. Down-regulation of APP in presynaptic GABAergic interneurons specifically suppressed GABAergic, but not glutamatergic, synaptic transmission strength and inputs onto both the somatic and dendritic compartments of hippocampal CA1 pyramidal neurons. Moreover, APP deletion manifested differential effects in somatostatin- and parvalbumin-positive interneurons in the hippocampal CA1, resulting in distinct alterations in inhibitory synapse numbers, transmission, and excitability. The infusion of MDGA1 MAM protein mimicked postsynaptic MDGA1 gain-of-function phenotypes that involve the presence of presynaptic APP. The overexpression of MDGA1 wild type or MAM, but not MAM-deleted MDGA1, in the hippocampal CA1 impaired novel object-recognition memory in mice. Thus, our results establish unique roles of APP–MDGA1 complexes in hippocampal neural circuits, providing unprecedented insight into *trans*-synaptic mechanisms underlying differential tuning of neuronal compartment-specific synaptic inhibition.

MDGA1 | amyloid precursor protein | synaptic inhibition | neural circuit | hippocampus

The spatial segregation of synapses and compartment-specific signaling pathways in neurons permits the encoding of input-specific synaptic plasticity, a fundamental feature of neural information processing in the central nervous system (CNS) (1). The neurochemical and functional consequences of synaptic inhibition in the hippocampus depend on differential innervation patterns, which in turn are dictated by various GABAergic interneurons (2–5). These distinct inhibition modes determine neuronal computation by controlling postsynaptic electrogenesis (6). The mechanisms of perisomatic and dendritic inhibition are highly diverse and heterogeneous, relying on the recruitment of different fast or non–fast-spiking interneurons (5). The proper establishment of this inhibition is essential for the operation of neural circuits, and its failure is linked to a number of neurodevelopmental disorders (7, 8).

Anatomical and electrophysiological distinctions between perisomatic and dendritic inhibition are well defined. Remarkably, however, the molecular underpinnings of these distinctions across brain areas have slowly unraveled. Neuroligin-2 (Nlgn2), a key GABAergic synapse-specific adhesion protein (9), and its binding proteins, gephyrin, collybistin, and $GABA_A$ receptor subunits (10, 11), form a select molecular apparatus in postsynaptic neurons that promotes perisomatic, but not dendritic, inhibition (12). Intriguingly, MDGA1 (meprin, A-5 protein, and receptor protein-tyrosine phosphatase mu [MAM] domain-containing glycosylphosphatidylinositol anchor protein 1) was recently proposed as a suppressive factor that contributes to perisomatic disinhibition (13).

MDGA1 is part of a two-member family of glycosylphosphatidylinositol-anchored proteins that plays a critical role at early steps in CNS development (13–15). MDGA1 *cis* interacts directly with and inhibits Nlgn2 by preventing its binding to presynaptic neurexins (Nrxns) (16, 17). Structural studies have elucidated key features underlying how MDGA1 negatively modulates Nlgn/Nrxn synaptic adhesion pathways (18–20), revealing that

Significance

This study demonstrates a universal synaptic mechanism responsible for tuning GABAergic neural circuit strength and turnover. These observations are relevant to the issue of neural circuit dynamics, which have only been investigated in certain limited contexts, particularly at a subset of glutamatergic neural circuits. Our work provides compelling evidence to support a crucial and unique physiological role for amyloid precursor protein (APP) in shaping GABAergic neural circuits. Our unequivocal demonstration of the physiological significance of MDGA1–APP complexes at specific hippocampal GABAergic neural circuits enables us to propose a conceptual framework that adds a striking twist to our understanding of the organization of mammalian inhibitory synapses in addition to unmasking a previously unidentified physiological role for APP proteins.

Author contributions: W.C.O. and J. Ko designed research; J. Kim, S. Kim, H.K., I.-W.H., S.B., S. Karki, D.K., R.O., G.B., J.Y.K., and W.C.O. performed research; D.K. and J.Y.K. contributed new reagents/analytic tools; J. Kim, S. Kim, H.K., I.-W.H., S.B., S. Karki, R.O., J.Y.K., T.K., J.W.U., W.C.O., and J. Ko analyzed data; and W.C.O. and J. Ko wrote the paper.

The authors declare no competing interest.

This article is a PNAS Direct Submission.

[1]J. Kim and S. Kim contributed equally to this work.

[2]H.K. and I.-W.H. contributed equally to this work.

[3]To whom correspondence may be addressed. Email: wonchan.oh@cuanschutz.edu or jaewonko@dgist.ac.kr.

This article contains supporting information online at http://www.pnas.org/lookup/suppl/doi:10.1073/pnas.2115326119/-/DCSupplemental.

Published January 24, 2022.

MDGA1-binding interfaces in Nlgns largely overlap with Nrxn-binding interfaces. Although MDGA1 localization in neurons was not clearly defined, the resolved MDGA1/Nlgn2 complex structure identified plausible *cis* interactions with Nlgn2, suggesting the postsynaptic localization of MDGA1 (20). In addition, results from MDGA1-knockout (KO) mice showed that MDGA1 deletion specifically increases perisomatic inhibition but suppresses long-term potentiation in hippocampal CA1 pyramidal neurons (21). Despite these intriguing observations obtained using constitutive MDGA1-KO mice, these prior studies have not demonstrated whether MDGA1 directly targets Nlgn2 to negatively regulate synaptic inhibition in vivo. To address this question, we sought to isolate additional MDGA1-binding proteins, identifying amyloid precursor protein (APP). To demonstrate a role for MDGA1–APP complexes in regulating the properties of GABAergic neural circuits of the hippocampal CA1, we performed MDGA1 gain-of-function and APP loss-of-function analyses. Collectively, our evidence suggests that MDGA1 "tunes" APP-mediated synaptic inhibition in the dendritic, but not somatic, compartment of hippocampal CA1 pyramidal neurons and targets APP (but not Nlgn2) in GABAergic neural circuits of the hippocampal CA1 in vivo.

Results

MDGA1 Directly Interacts with APP. To identify additional ligand(s) for MDGA1 in vivo, we performed affinity chromatography of adult (postnatal day 42 [P42]) mouse brain synaptosomes using recombinant MDGA1-Fc purified from supernatants of human embryonic kidney 293T (HEK293T) cells transfected with an expression vector encoding MDGA1 extracellular domains fused to human Fc (*SI Appendix*, Fig. S1*A*) followed by mass spectrometry (MS) analyses (Fig. 1 *A*–*C*). In addition to various peptides encoding Nlgn isoforms, APP was identified among many identified peptides (*SI Appendix*, Table S1). To validate these MS results, we performed cell-surface–binding assays to assess the binding of recombinant MDGA1-Fc to HEK293T cells expressing hemagglutinin (HA)-tagged APP family members (APP, amyloid precursor-like protein 1 [APLP1], and APLP2) (Fig. 1 *D* and *E*). MDGA1-Fc, but not Fc alone (negative control), robustly bound to APP- or APLP2-expressing, but not APLP1-expressing, cells (Fig. 1 *D* and *E*). MDGA1 bound to APP in an extracellular Ca^{2+}-dependent manner as evidenced by the treatment with the Ca^{2+} chelator ethylene glycol tetraacetic acid (10 mM) (*SI Appendix*, Fig. S1 *G* and *H*). The coimmunoprecipitation analyses using lysates from cultured hippocampal neurons or detergent-solubilized juvenile (P14) or adult (P70) mouse membrane fractions with APP antibodies (clone Y188) showed the formation of an APP–MDGA1 complex in vivo (Fig. 1*F*; see *SI Appendix*, Fig. S1 *B*–*F* for validation of MDGA antibodies). However, MDGA2-Fc did not bind to APP in HEK293T or brain pull-down assays (*SI Appendix*, Fig. S1 *I* and *J*). To exclude the possibility that intermediate(s) expressed in HEK293T cells might bridge indirect associations of MDGA1 with APP and show that His-HA-APP binds directly to recombinant MDGA1, we performed binding assays using purified recombinant His-HA-APP and MDGA1-Fc (Fig. 1*G*). To this end, we expressed full-length HA-APP on the surface of HEK293T cells, incubated these cells (or control HEK293T cells) with increasing amounts of MDGA1-Fc, measured cell-surface–bound proteins using horseradish peroxidase–tagged secondary antibodies, and performed Scatchard analyses to calculate binding affinity. These analyses yielded an apparent dissociation constant (K_d) of 84.74 nM for MDGA1-Fc toward APP expressed on the cell surface (Fig. 1*H*). Taken together, these results indicate that MDGA1 binds selectively to APP with nanomolar affinity.

The Extension Domain of APP Binds to MDGA1. To determine which APP domains interact with MDGA1, we performed cell-surface–binding assays using constructs expressing various functional APP domains (Fig. 1*I*). We utilized the APP_{695} spliced isoform because it is a predominant neuronal form expressed in the CNS (22). Remarkably, MDGA1-Fc bound robustly to the surface of cells expressing the extension domain (ExD) of APP but did not exhibit significant binding to cells expressing the E1 domain (composed of the growth factor–like domain and copper-binding domain), the acidic region (AcD), the E2 domain, or the juxtamembrane region (Fig. 1 *J* and *K*). We also investigated whether mutations in APP linked to Alzheimer's disease (AD) affect interactions with MDGA1, randomly selecting a subset of AD-associated APP variants (S198P, A201V, A673T [Icelandic], E693G [Arctic], D694N [Iowa], and I716V [Florida]) for examination (archived from ALZFORUM; https://www.alzforum.org). We found that none of the tested APP mutations affected binding to MDGA1 (*SI Appendix*, Fig. S2), in keeping with the fact that pathogenic APP mutations are near β- and γ-secretase cleavage sites (23). Moreover, the S198P mutation located in the APP ExD (APP^{S198P}), found in people afflicted with AD (24), did not affect binding to MDGA1 (*SI Appendix*, Fig. S2). We further subdivided the APP ExD into Ex1 and Ex2 to map the minimal MDGA1-binding site, noting that a 24–amino acid sequence encompassing Ex2 residues is responsible for binding to the sushi domain of γ-aminobutyric acid type B receptor subunit 1a ($GABA_BR1a$) (25, 26) (Fig. 1 *I*, *Inset*). Given that other APP family members (APLP1 and APLP2) are reported to lack a defined ExD domain (27), the fact that MDGA1-Fc bound to APLP2 suggests that domain(s) other than those involved in binding of MDGA1 to APP may contribute to APLP2 binding to MDGA1. Indeed, MDGA1-Fc bound to the E2 domain as well as the AcD of APLP2 (*SI Appendix*, Fig. S3 *A*–*C*), which is ∼54.6% similar to APP AcD (including ExD, which is uniquely present in APP) but only shows ∼17.8% similarity to APLP1 AcD (27). The coimmunoprecipitation analyses of P14 and P70 mouse membrane fractions showed nondetectable APLP2–MDGA1 complexes in vivo (*SI Appendix*, Fig. S3*D*). Taken together, our results suggest that MDGA1 preferentially forms complexes with APP compared with APLP2 in vivo.

A Short Peptide within the APP ExD Binds to Both MDGA1 and $GABA_BR1$. To further identify the minimal binding region within APP Ex2, we produced various APP-Fc proteins that collectively entirely covered the Ex2 region (designated APP Ex2-1 to APP Ex2-9; *SI Appendix*, Fig. S4*A*) and tested whether they bound to cells expressing HA-MDGA1 or the HA-$GABA_BR1a$ sushi 1 domain (*SI Appendix*, Fig. S4 *B* and *C*). APP Ex2-1 (amino acids [aa] 204 to 220 of APP_{695}) and APP Ex2-3 [aa 204 to 212; previously identified to bind to $GABA_BR1a$ (26)] also bound to MDGA1, whereas APP Ex2-2 (aa 221 to 227) and APP Ex2-4 (aa 213 to 220) failed to bind both MDGA1 and $GABA_BR1a$ (*SI Appendix*, Fig. S4 *B* and *C*). Further analyses with APP Ex2-5 (aa 204 to 216), APP Ex 2-6 (aa 208 to 220), APP Ex2-8 (aa 204 to 207), and APP Ex2-9 (aa 217 to 220) suggested that the "VWWGGADTD" sequence is necessary and sufficient for binding of APP to both MDGA1 and $GABA_BR1a$ (*SI Appendix*, Fig. S4). Further deletion of the C-terminal "ADTD" sequence (APP Ex 2-7; aa 208 to 212) drastically diminished but did not entirely eliminate APP binding to both MDGA1 and $GABA_BR1a$ (*SI Appendix*, Fig. S4). Overall, these results suggest that MDGA1 binds to a specific peptide sequence within APP ExD that completely overlaps with the reported $GABA_BR1a$-binding site.

APP Binds to the MAM Domain of MDGA1. Next, to determine which MDGA1 domains interact with APP, we performed cell-surface–binding assays using constructs expressing various functional MDGA1 domains (Fig. 1*L*). Strikingly, APP ExD-Fc

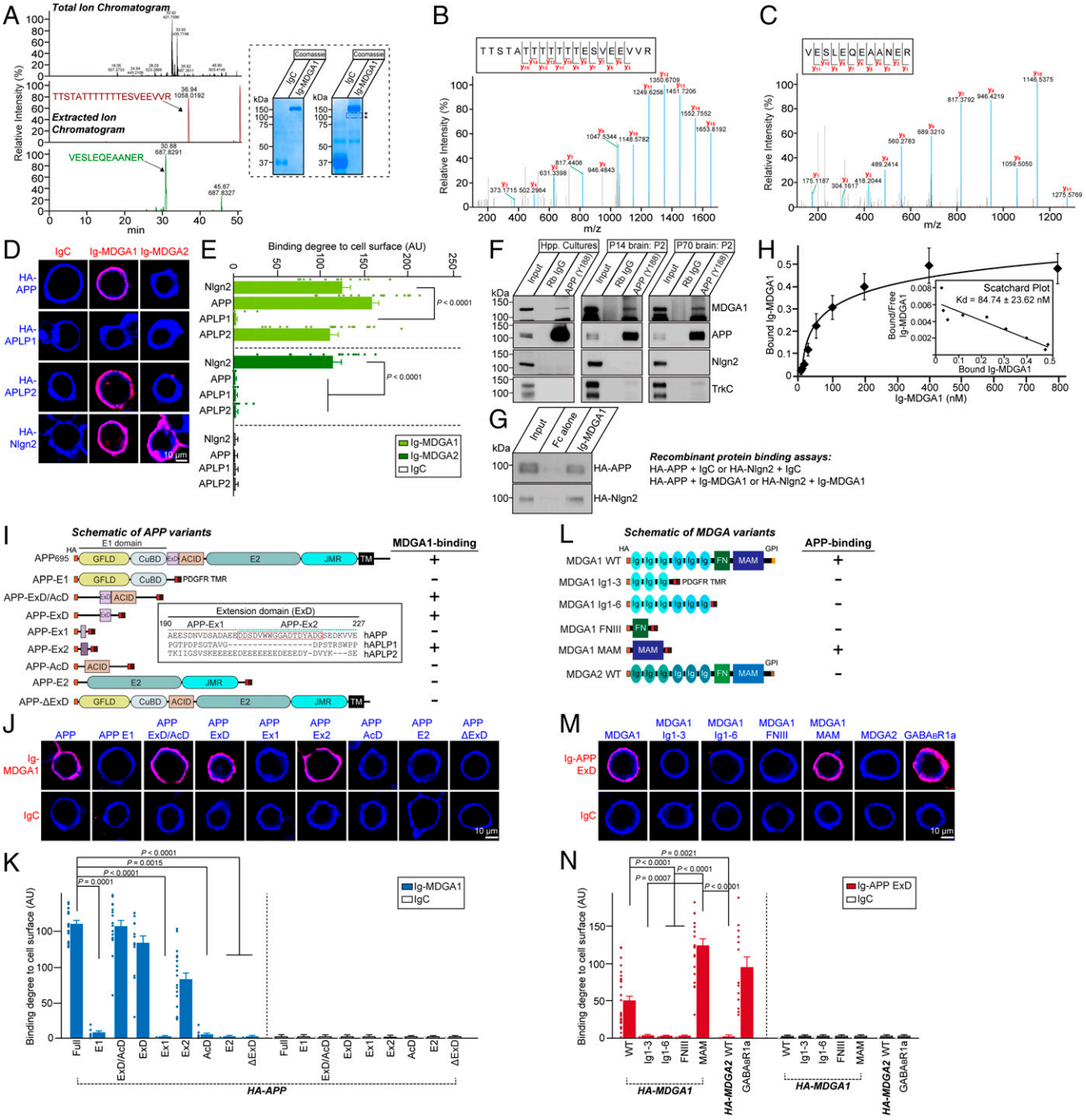

Fig. 1. APP is a putative binding protein for MDGA1. (*A*) Total ion chromatogram of tryptic digests of Ig-MDGA1–bound eluates separated by liquid chromatography (LC) and extracted ion chromatograms of *m/z* 1,058.02 ion and 687.83 ion generated from mouse APP. Coomassie blue-stained gel showing recombinant Ig-control and Ig-MDGA1 fusion proteins used for affinity chromatography (*Left*) and distinct bands corresponding to proteins purified on immobilized MDGA1 and subjected to MS (*Right*). An asterisk indicates a specific band unique to the Ig-MDGA1–bound fraction. (*B* and *C*) Spectra of two double-charged peptides unique to mouse APP at *m/z* 1,058.02 (36.94 min) and 687.83 (30.88 min), respectively, obtained by LC-MS/MS and identified by y-ions as peptides with the aa sequences TTSTATTTTTTTESVEEVVR (aa 268 to 288) and VESLEQEAANER (aa 438 to 450). (*D*) Cell-surface–binding assays. HEK293T cells expressing HA-APP, HA-APLP1, HA-APLP2, or HA-Nlgn2 were incubated with control IgC, Ig-MDGA1, or Ig-MDGA2 and analyzed for Ig-fusion proteins (red) and HA (blue) by immunofluorescence imaging. (*E*) Quantification of cell-surface–binding in *D*. (*F*) Analysis of complex formation of APP with MDGA1, Nlgn2, and TrkC by coimmunoprecipitation using lysates of cultured hippocampal neurons (*Left*) or hippocampal lysates from P14 (*Middle*) or P70 (*Right*) mice. Input, 1%. (*G*) Direct binding assays using purified Ig-MDGA1, HA-APP, and HA-Nlgn2 proteins. (*H*) Saturation binding of Ig-MDGA1 to HEK293T cells expressing HA-APP. (*Inset*) Scatchard plot generated by linear regression of the data; K_d was calculated from three independent experiments. (*I*) Diagrams of APP deletion variants used in cell-surface–binding assays. (*J*) Cell-surface–binding assays. HEK293T cells expressing the indicated HA-APP variants were incubated with control IgC or Ig-MDGA1 and analyzed for Ig-fusion proteins (red) and HA (blue) by immunofluorescence imaging. (*K*) Quantification of cell-surface binding in *J*. (*L*) Diagrams of MDGA1 deletion variants used in cell-surface–binding assays. (*M*) Cell-surface–binding assays. HEK293T cells expressing the indicated HA-MDGA1 variants were incubated with control IgC or Ig-APP-ExD and analyzed for Ig-fusion proteins (red) and HA (blue) by immunofluorescence imaging. (*N*) Quantification of cell-surface–binding in *M*. Error bars denote SEM. *P* values determined by Kruskal–Wallis test followed by Dunn's multiple comparison test (*E*, *K*, and *N*). See Dataset S1 for additional statistics.

bound to the surface of cells expressing the MAM domain of MDGA1 but not to those expressing Ig domains or FNIII repeat (Fig. 1 *M* and *N*). The measurement of binding affinity between MDGA1 MAM-Fc and APP revealed a K_d of 41.28 nM (*SI Appendix*, Fig. S5*A*), similar to the binding affinity between MDGA1-Fc and APP (Fig. 1*H*). Pull-down assays using APP ExD-Fc against lysates from HEK293T cells and detergent-solubilized mouse membrane fractions showed that APP ExD-Fc captured MDGA1 but not MDGA2 (*SI Appendix*, Fig. S5 *B* and *C*). Thus, APP ExD is necessary and sufficient for MDGA1 binding. Consistent with this, the recombinant MDGA1 MAM domain fused to Fc (MDGA1 MAM-Fc) bound to cells expressing HA-APP or HA-APLP2 but not to those expressing HA-Nlgn2 (*SI Appendix*, Fig. S5 *D* and *E*). In keeping with the observed absence of MDGA2 binding to APP (*SI Appendix*, Fig. S1), there is only ∼55.8% identity between the human MDGA1 MAM domain and human MDGA2 MAM domain and no clear sequence similarity with the MAM domains of other proteins (*SI Appendix*, Fig. S5 *F* and *G*). The MAM domain generally contains four conserved cysteine residues, also present in MDGA1 and MDGA2, that are often involved in forming disulfide-linked oligomers (28, 29). Small-angle X-ray scattering analyses showed that the MDGA1 MAM domain is monomeric, unlike other MAM domains (30–32) (*SI Appendix*, Fig. S5 *H–J*), and structural modeling revealed that these MDGA1 MAM mutations might disrupt the monomeric structure (*SI Appendix*, Fig. S5*K*). Thus, we tested whether the mutation of these cysteine residues in the MDGA1 MAM domain to alanine affects APP binding and found that APP ExD-Fc failed to bind to the MDGA1 MAM (C754A/C762A/C834A/C917A) mutant (*SI Appendix*, Fig. S5 *L* and *M*). We also found that β-site APP cleaving enzyme 1 –mediated cleavage of the MDGA1 MAM domain did not influence APP binding (33) (*SI Appendix*, Fig. S5 *N* and *O*). Taken together, our results indicate that the MDGA1 MAM domain is necessary and sufficient for binding to APP ExD.

MDGA1 Negatively Regulates GABAergic Synapse Maintenance through Binding to APP. We next assessed whether MDGA1 exerts its negative regulation of GABAergic synapse maintenance through binding to ligands (e.g., Nlgn2 or APP). We chose the hippocampal CA1 GABAergic circuits for this purpose for two reasons. First, hippocampal GABAergic neural circuits have been most extensively studied and established in the CA1 region (34). Second, key observations from MDGA1 gain-of-function and loss-of-function studies were obtained from experiments using either hippocampal cultures or hippocampal CA1 pyramidal neurons (16, 17, 21, 35). To determine cell-autonomous, postsynapse-specific effects of MDGA1 overexpression, we employed biolistic transfection of organotypic hippocampal slices (36). This approach allows for pairwise, internally controlled comparisons of the consequences of MDGA1 manipulations that are restricted to postsynaptic CA1 pyramidal neurons. We transfected neurons in hippocampal CA1 slice cultures with MDGA1 wild type (WT) or either of two MDGA1 mutants: MDGA1 ABC Mut, which introduces a subset of point mutations that abolish Nlgn2 binding (18), and MDGA1 ΔMAM, a MAM domain-deleted construct; we then conducted two-photon imaging and electrophysiology experiments (Fig. 2). Consistent with prior reports performed in dissociated cultured neurons (16, 17), the overexpression of MDGA1 WT attenuated gephyrin puncta density by ∼30% in the distal dendrites of transfected hippocampal CA1 neurons without affecting excitatory synapses (Fig. 2 *A–E*). Surprisingly, the overexpression of MDGA1 ABC Mut effectively decreased gephyrin puncta density by ∼20% in the distal dendrites of the transfected neurons, whereas the overexpression of MDGA1 ΔMAM failed to do so (Fig. 2*B*), indicating that MDGA1 requires MAM domain-mediated interactions with APP for its negative action in hippocampal CA1 GABAergic synapses. In addition, the overexpression of MDGA1 WT or ABC Mut, but not MDGA1 ΔMAM, potently suppressed frequency of miniature inhibitory postsynaptic currents (mIPSCs) (Fig. 2 *F–I*). Similar MDGA1 overexpression effects were observed for evoked inhibitory postsynaptic currents (eIPSCs) with MDGA1 WT or ABC Mut, but not MDGA1 ΔMAM, negatively regulating inhibitory synaptic strength (Fig. 2 *J–O*). Notably, MDGA1-mediated suppressive effects on eIPSCs were confined to the distal dendritic, but not the somatic or proximal dendritic, compartment in hippocampal CA1 pyramidal neurons (Fig. 2 *J–O*). We next attempted to determine whether conditional deletion of MDGA1 exerts anatomical and/or functional effects on mature GABAergic synapses in hippocampal CA1 neurons (*SI Appendix*, Fig. S6). Unexpectedly, and in stark contrast to the results obtained from MDGA1 constitutive KO mice (21), we found no alterations in mIPSCs and somatic eIPSCs in hippocampal CA1-specific *Mdga1*-cKO (conditional knockout) mice (*SI Appendix*, Fig. S6 *H–P*). However, the puncta density of vesicular GABA transporter (VGAT), a marker for presynaptic GABAergic nerve terminals, was significantly increased in the stratum lacunosum-moleculare (SLM) layer of young adult *Mdga1*-cKO mice (*SI Appendix*, Fig. S6 *D–G*). In agreement with this anatomical phenotype, the distal dendritic IPSC amplitudes were also increased in young adult *Mdga1*-cKO mice (*SI Appendix*, Fig. S6 *Q–S*). These results suggest that postsynaptic MDGA1 negatively regulates GABAergic synapses on distal dendrites of pyramidal neurons, an action that requires interactions with APP via the MAM domain.

Presynaptic APP Is Required for GABAergic Synapse Maintenance in the Hippocampal CA1, Independent of MDGA1 Binding to APP ExD. APP is strongly expressed in both excitatory and inhibitory neurons (37–39), whereas MDGA1 is primarily expressed in excitatory neurons of the hippocampal CA1 region (16, 21). Although an APP deficiency is known to impact GABAergic synapse signaling (40, 41), the mechanism regulating APP-mediated synaptic inhibition has not been well elucidated. To investigate the function of APP–MDGA1 complexes at GABAergic synapses, we first generated lentiviral constructs expressing short hairpin RNA (shRNA) targeting APP (APP shRNA) and validated its efficacy in the specific knockdown (KD) of APP levels in mouse cultured hippocampal neurons (*SI Appendix*, Fig. S7 *A–C*). APP shRNA decreased APP protein levels by ∼83% and *App* messenger RNA levels by 85% without affecting *Aplp1* or *Aplp2* levels (*SI Appendix*, Fig. S7 *A–C*). Moreover, immunohistochemistry experiments consistently confirmed this KD efficacy in mouse brains (*SI Appendix*, Fig. S7 *D* and *E*). To determine whether APP deletion affects GABAergic synapse formation/development, we employed an organotypic slice culture system (36). Using two-photon laser-scanning microscopy, we analyzed the number and size of gephyrin puncta along dendrites of CA1 pyramidal neurons in organotypic slices ∼3 wk after viral infection with adeno-associated viruses (AAVs) expressing short hairpin APP (shAPP) (Fig. 3*A*). Strikingly, the density but not size of gephyrin puncta was significantly reduced on the distal dendrites of CA1 pyramidal neurons in APP-deficient hippocampal slices (Fig. 3 *C–E*). Two-photon imaging combined with measurements of two-photon GABA uncaging-evoked IPSCs confirmed the absence of structural and functional alterations of individual inhibitory synapses on CA1 pyramidal neurons (Fig. 3 *F* and *G*). Electrophysiological recordings of mIPSCs revealed that APP deletion specifically decreased the frequency but not amplitude of mIPSCs (Fig. 3*H*). To discriminate the locus of APP deletion effects (i.e., pre- versus postsynaptic neurons), we employed the biolistic transfection of shAPP in organotypic

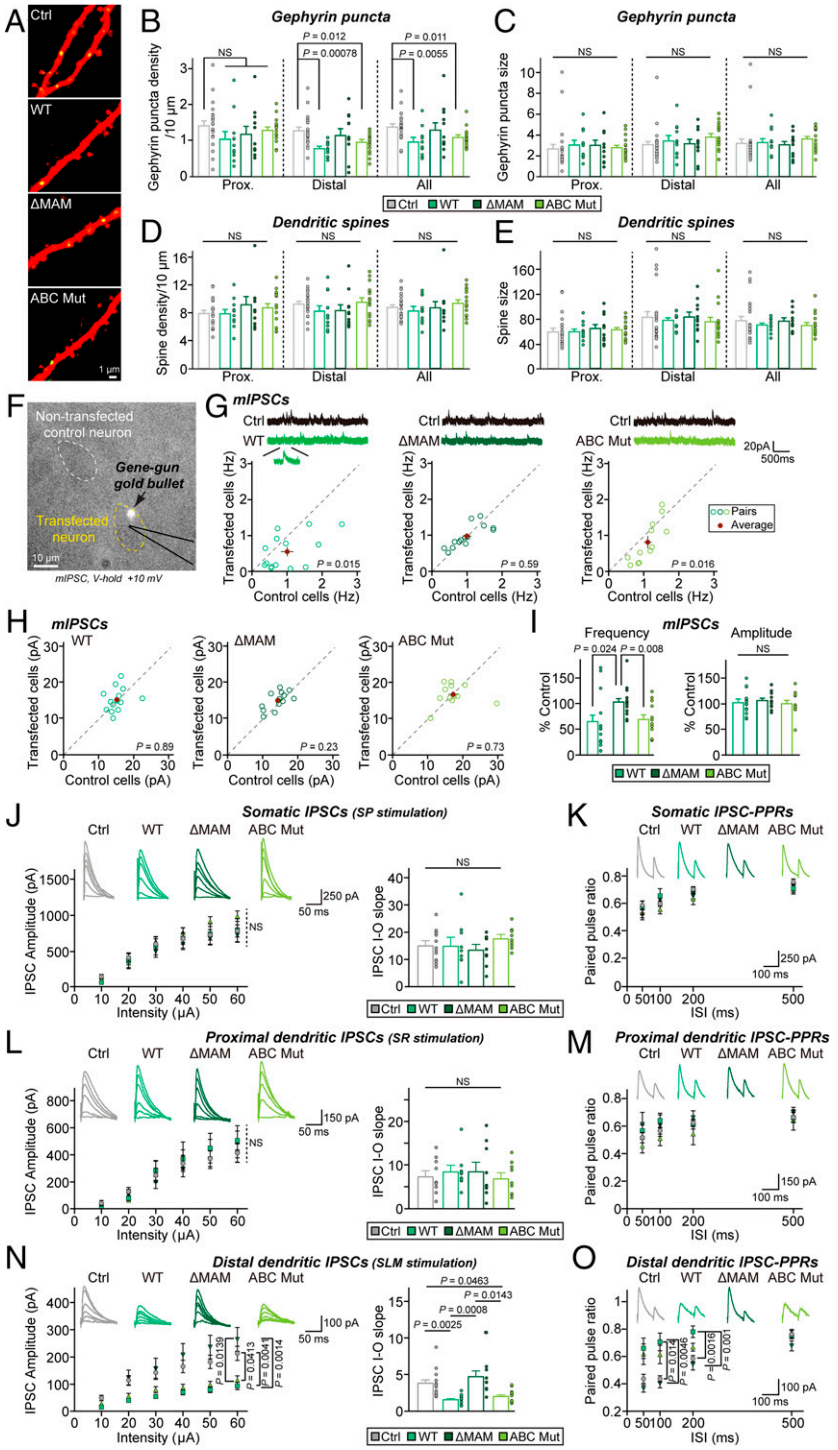

Fig. 2. MDGA1 negatively regulates dendritic inhibition via the APP-binding MAM domain. (*A*) Two-photon images of dendritic segments from hippocampal CA1 pyramidal neurons expressing the indicated MDGA1 variants, tdTomato, and gephyrin intrabody-GFP. (*B–E*) Quantitative analysis of gephyrin puncta density (*B*) and size (*C*) and spine density (*D*) and size (*E*) from proximal, distal, and all dendrites of CA1 pyramidal neurons at EP21–25. (*F*) Differential inteference contrast image of an organotypic hippocampal slice culture showing a whole-cell recording from a hippocampal CA1 pyramidal neuron transfected with a specific MDGA1 variant (indicated by a gold bullet) and its neighboring nontransfected control neuron. Each cell is delineated by a dotted circle. (*G–I*) Representative mIPSC traces from nontransfected cells (*Top*) and cells transfected with the indicated MDGA1 construct (*Bottom*) (*G*). Scatter plots showing the frequency (*G*) and amplitude (*H*) of mIPSCs from pairs of specific MDGA1 construct-transfected and control cells. Quantitative analysis (*I*) of the frequency (*Left*) and amplitude (*Right*) of mIPSCs compared with controls at EP19–24. (*J*) Representative somatic eIPSC trace, average eIPSC I-O curve (*Left*), and average eIPSC I-O slope (*Right*) for hippocampal CA1 pyramidal neurons from mice expressing control (gray), MDGA1 WT (green), MDGA1 ΔMAM (deep green), or MDGA1 ABC Mut (light green). (*K*) Representative somatic eIPSC paired-pulse ratio (PPR) traces and average PPR. (*L*) Representative proximal dendritic eIPSC traces, average eIPSC I-O curve (*Left*), and average eIPSC I-O slope (*Right*). (*M*) Representative proximal dendritic PPR traces and average PPR. (*N*) Representative distal dendritic eIPSC traces, average eIPSC I-O curve (*Left*) and average eIPSC I-O slope (*Right*). (*O*) Representative distal dendritic PPR traces and average PPR. Error bars denote SEM. *P* values determined by Student's two-tailed *t* test (*B–E* and *G–I*) or Kruskal–Wallis test followed by Dunn's multiple comparison test (*J–O*). See Dataset S1 for additional statistics. NS, not significant.

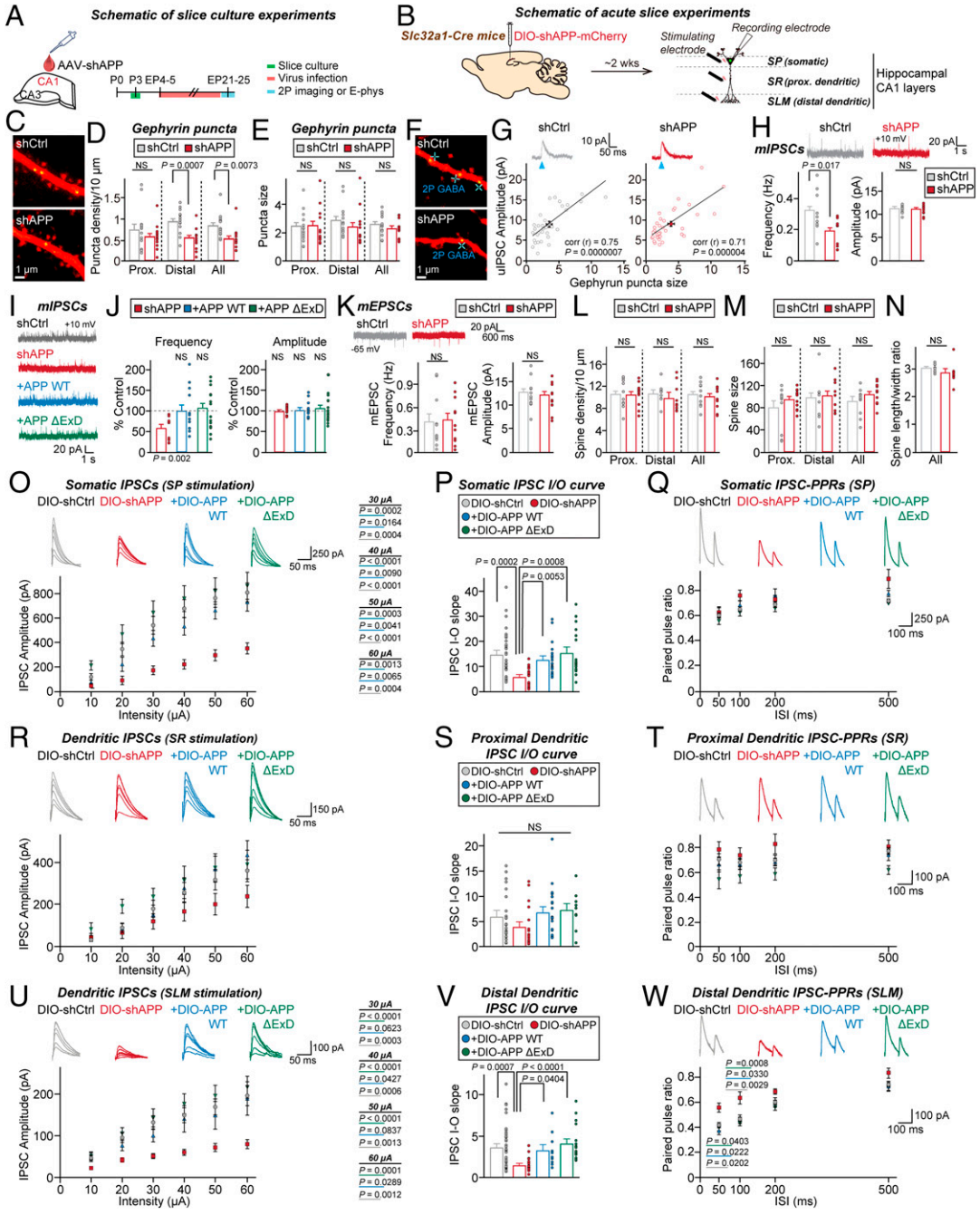

Fig. 3. Presynaptic APP in hippocampal CA1 GABAergic interneurons is required for synaptic inhibition. (*A*) Schematic showing AAV–shAPP infection at EP4–5 and imaging and recording from hippocampal organotypic slices at EP21–25. (*B*) Schematic showing DIO–shAPP in vivo injection into the hippocampal CA1 and recording at CA1 pyramidal neurons with different locations of the stimulating electrode. (*C*) Two-photon images of dendritic segments of tdTomato and gephyrin intrabody-GFP cotransfected CA1 pyramidal neurons in AAV-shCtrl– or AAV-shAPP–expressing hippocampal slices. (*D* and *E*) Quantitative analysis of gephyrin puncta density (*D*) and size (*E*) in proximal, distal, and all dendrites at EP21–25. (*F*) Two-photon images of dendrites showing gephyrin puncta on CA1 pyramidal neurons in AAV-shCtrl– or AAV-shAPP–expressing hippocampal slices. Individual gephyrin puncta were exposed to two-photon GABA uncaging test pulses (blue crosses, 8 to 10 trials at 0.1 Hz). (*G*) Uncaging-evoked IPSCs (uIPSCs) evoked by GABA uncaging, measured in whole-cell voltage-clamp mode at +10 mV. Arrowheads indicate onset of GABA uncaging. uIPSC amplitude plotted against gephyrin puncta size from shCtrl and shAPP groups. (*H*) Traces of mIPSCs measured by whole-cell patch-clamp recordings in AAV-shCtrl–expressing (gray) or AAV-shAPP–expressing (red) slices. Quantitative analyses of the frequency and amplitude of mIPSCs. (*I* and *J*) mIPSC traces (*I*) in AAV-shCtrl–expressing (gray), AAV-shAPP–expressing (red), +AAV-APP WT–expressing (blue), or +AAV-APP ΔExD–expressing (green) slices. Quantitative analyses (*J*) of the mIPSC frequency and amplitude of each group compared with their respective controls. (*K*–*N*) mEPSCs traces (*K*) measured by whole-cell patch-clamp recordings at −65 mV in AAV-shCtrl–expressing (gray) or AAV-shAPP–expressing (red) slices. Quantitative analyses (*K*) of the frequency and amplitude of mEPSCs. Summary graphs of spine density (*L*), spine size (*M*), and length/width ratio (*N*) from proximal, distal, and all dendrites of CA1 pyramidal neurons. (*O* and *P*) Representative somatic eIPSC traces, average eIPSC I-O curve (*O*), and average eIPSC I-O slope (*P*) from hippocampal CA1 pyramidal neurons from *Slc32a1*-Cre mice expressing DIO–shCtrl (gray), DIO–shAPP (red), DIO–shAPP + DIO–APP WT (blue), or DIO–shAPP + DIO–APP ΔExD (green). (*Q*) Representative somatic eIPSC PPR traces and average PPR. (*R* and *S*) Representative proximal dendritic eIPSC traces, average eIPSC I-O curve (*R*) and average eIPSC I-O slope (*S*). (*T*) Representative proximal dendritic eIPSC PPR traces and average PPR. (*U* and *V*) Representative distal dendritic eIPSC traces, average eIPSC I-O curve (*U*), and average eIPSC I-O slope (*V*). (*W*) Representative distal dendritic eIPSC PPR traces and average PPR. Error bars denote SEM. *P* values determined by two-tailed Student's *t* test (*D*, *E*, *G*, *H*, *K*, *L*, and *N*) or Kruskal–Wallis test followed by Dunn's multiple comparison test (*J*, *P*, *Q*, *S*, *T*, *V*, and *W*). See Dataset S1 for additional statistics. NS, not significant.

hippocampal slices and found no effects on either GABAergic or glutamatergic synapses on pyramidal neurons (*SI Appendix*, Fig. S8 *A–F*), indicating a more pronounced presynaptic function of APP in inhibitory synapse maintenance. Neither functional nor structural alterations were observed at excitatory synapses of CA1 pyramidal neurons in APP-deficient hippocampal slices (Fig. 3 *K–N*), suggesting a specific role of APP at GABAergic synapses in the hippocampal CA1 area. We then asked whether the decrease in the mIPSC frequency could be reversed by the expression of APP WT or the ExD-deleted APP mutant (APP ΔExD). To this end, we superinfected shAPP-expressing hippocampal slices at EP6–7 with AAV–APP WT or AAV–APP ΔExD and measured mIPSCs. We found that both APP WT and APP ΔExD rescued the decreased mIPSC frequency without affecting mIPSC amplitude (Fig. 3 *I* and *J*). We next infused AAVs expressing Cre-dependent APP shRNA (AAV–double-floxed inverse open reading frame [DIO]–shAPP) into the hippocampal CA1 area of *Vgat* (*Slc32a1*)-ires-Cre mice (*SI Appendix*, Fig. S8 *G* and *H*; see *SI Appendix*, Fig. S7 *F* and *G* for validation of AAV–DIO–shAPP). The selective deletion of APP in GABAergic interneurons of the hippocampal CA1 markedly attenuated VGAT puncta density in all layers of the hippocampal CA1 area (*SI Appendix*, Fig. S8 *G* and *H*). The introduction of either APP WT or APP ΔExD completely rescued VGAT puncta, restoring VGAT puncta density to control levels (*SI Appendix*, Fig. S8 *G* and *H*). To corroborate these observations, we recorded eIPSCs monosynaptically in hippocampal CA1 pyramidal neurons receiving projections from either APP-deficient GABAergic terminals or control terminals (Fig. 3 *B* and *O–W*). APP deletion in hippocampal CA1 GABAergic interneurons significantly decreased both somatic and distal dendritic inhibition in pyramidal neurons (Fig. 3 *O–W*). Remarkably, the reduced amplitudes of distal dendritic but not somatic or proximal dendritic eIPSCs in CA1 neurons receiving projections from APP-deficient terminals were rescued by selective expression of APP WT or APP ΔExD (Fig. 3 *O–W*). The deletion of APLP2 in hippocampal CA1 GABAergic interneurons did not alter the density or size of VGAT puncta (*SI Appendix*, Fig. S3 *E* and *F*). These results suggest that APP contributes to the regulation of synaptic inhibition in both somatic and distal dendritic compartments of hippocampal CA1 pyramidal neurons, and APP ExD is not required for the execution of GABAergic synaptic functions; this latter finding contrasts with the critical role of APP ExD in regulating $GABA_BR1a$ function in modulating "excitatory" synaptic transmission (26).

APP Is Required for Excitability in Parvalbumin and Somatostatin Interneurons and Controls Neurotransmitter Release. APP is reported to be highly expressed in a variety of GABAergic interneurons in the hippocampal CA1 region (39). Consistent with this, we observed a high endogenous expression of APP in both somatostatin $(SST)^+$ and parvalbumin $(PV)^+$ interneurons (*SI Appendix*, Fig. S7 *H–J*). We next assessed the effects of knocking down APP by stereotactically injecting AAV–DIO–shAPP into *Sst*–ires–Cre (SST–Cre) mice or *Pvalb*–Cre (PV–Cre) and quantifying the total density of $VGAT^+$ or $GABA_AR\gamma2^+$ puncta in all layers of the hippocampal CA1 region (*SI Appendix*, Figs. S9 *A–C* and S10 *A–C*). Strikingly, we observed a profound decrease in the density of $VGAT^+$ or $GABA_AR\gamma2^+$ synaptic puncta in the SLM layer of SST–Cre mice injected with AAV–DIO–shAPP compared to control mice injected with AAVs expressing nontargeting shRNAs (*SI Appendix*, Fig. S9 *A–C*). There were no alterations in the density of $VGAT^+$ or $GABA_AR\gamma2^+$ synaptic puncta in any examined hippocampal CA1 layers of PV–Cre mice injected with AAV–DIO–shAPP (*SI Appendix*, Fig. S9 *A–C*), suggesting that APP is specifically required for the maintenance of selective synaptic inputs derived from SST^+ interneurons (but not those from PV^+ interneurons). To test whether the loss of APP in GABAergic interneurons impairs specific synaptic properties, we sought to selectively mark and manipulate SST^+ or PV^+ neurons (*SI Appendix*, Figs. S9 *D* and *I* and S10 *D* and *I*). We delivered AAV–DIO–shAPP–mCherry and AAV–DIO–ChR2–enhanced green fluorescent protein (EGFP) into the hippocampal CA1 in SST–Cre mice (*SI Appendix*, Fig. S9 *D* and *I*) or PV–Cre (*SI Appendix*, Fig. S10 *D* and *I*). We identified SST^+ or PV^+ neurons expressing both AAVs (yellow, reflecting overlapping expression of mCherry and EGFP) in the hippocampal CA1 area 2 wk postinjection (*SI Appendix*, Figs. S9 *D* and *I* and S10 *D* and *I*). The targeted photostimulation of optical fibers revealed optically evoked IPSCs (oIPSCs) in the indicated GABAergic interneurons in acute brain slices from SST–Cre and PV–Cre mice. In response to current injections, the patched SST^+ neurons exhibited low-threshold spiking, whereas PV^+ neurons exhibited fast-spiking properties (*SI Appendix*, Figs. S9*J* and S10*J*). We found that oIPSCs elicited by the stimulation of APP-deficient SST^+ or PV^+ neurons were decreased by ∼58 and ∼53%, respectively (*SI Appendix*, Figs. S9 *E* and *F* and S10 *E* and *F*). However, paired-pulse ratios were significantly enhanced in APP-deficient SST^+ neurons, increasing by ∼10%, but were not changed in APP-deficient PV^+ neurons (*SI Appendix*, Figs. S9 *G* and *H* and S10 *G* and *H*). Moreover, latency of oIPSCs were significantly slower in APP-deficient SST^+ neurons (*SI Appendix*, Figs. S9*F* and S10*F*). Intrinsic neuronal excitability was markedly reduced in APP-deficient SST^+ and PV^+ neurons without changes in resting membrane potential. Indeed, the minimal current that elicited an action potential (i.e., rheobase) was significantly increased (*SI Appendix*, Figs. S9 *K–M* and S10 *K–M*). Consistent with prior results from APP-deficient hippocampal CA1 slices (Fig. 3 *C–E*), there was a specific reduction in gephyrin puncta density at CA1 pyramidal neuron synapses formed by APP-deficient SST^+ or PV^+ neurons in organotypic slices (*SI Appendix*, Figs. S9 *N–S* and S10 *N–S*). The absence of robust phenotypes in APP-deficient PV^+ neurons would appear to be inconsistent with the strong phenotypes in APP-deficient GABAergic interneurons (Fig. 3). However, it is possible that APP expressed in other interneurons (e.g., CCK^+ interneurons) could provide somatic inhibition in the hippocampal CA1 (5). Taken together, these results demonstrate that APP deficiency in hippocampal CA1 interneurons leads to differential alterations in inhibitory synaptic strength and release probability, resulting in a lower density of inhibitory synapses on pyramidal neurons.

MDGA1 MAM Suppresses GABAergic Synaptic Transmission and Synapse Stabilization. APP Ex2-3 (also known as APP 17-mer) was reported to suppress both excitatory and inhibitory synaptic transmission in a $GABA_BR$ activity-dependent manner in mature cultured hippocampal neurons (26) and was found to bind to both $GABA_BR1a$ and MDGA1 (*SI Appendix*, Fig. S3). Thus, instead of using the APP 17-mer, we employed the purified MDGA1 MAM protein as a tool for probing the role of APP–MDGA1 complexes in controlling GABAergic synapse properties in hippocampal CA1 neurons. We first tested whether MDGA1 MAM could alter the GABAergic synaptic transmission in acute hippocampal CA1 slices (Fig. 4*A* and *SI Appendix*, Fig. S11*A*). The application of MDGA1 MAM (750 nM and 1 μM) significantly reduced the mIPSC frequency in a concentration-dependent manner (Fig. 4 *B* and *C* and *SI Appendix*, Fig. S11*A*). Moreover, treatment with 1 μM MDGA1 MAM did not affect the miniature excitatory postsynaptic current (mEPSC) frequency; the application of the same concentration of MDGA2 MAM did not alter either the mEPSC or mIPSC frequency (Fig. 4 *B* and *C* and *SI Appendix*, Fig. S11 *A–D*). In line with these results, the interaction of APP with MDGA1 in hippocampal CA1 slices was slightly decreased by treatment with 1 μM

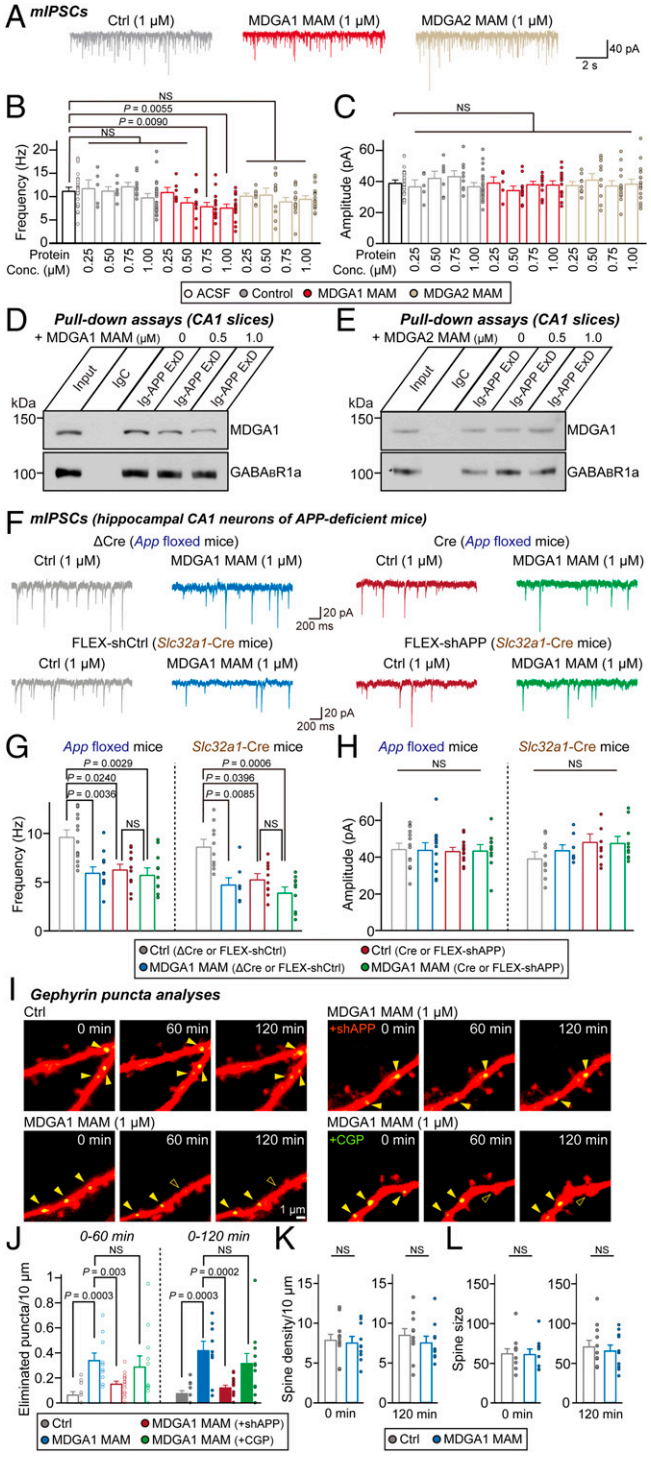

Fig. 4. MDGA1 MAM facilitates GABAergic synapse elimination in hippocampal CA1 neurons. (*A*) Representative mIPSC traces from hippocampal CA1 pyramidal neurons treated with 1 μM Fc protein (gray), 1 μM MDGA1 MAM (red), or 1 μM MDGA2 MAM (beige) for 1 h. (*B* and *C*) Average mIPSC frequency (*B*) and amplitude (*C*). (*D* and *E*) Effects of the indicated concentrations of MDGA1 MAM (*D*) or MDGA2 MAM (*E*) on complex formation of APP with MDGA1 or $GABA_BR1a$ in the hippocampal CA1. Input, 1%. (*F*) Representative mIPSC traces from hippocampal CA1 pyramidal neurons from $App^{f/f}$ (ΔCre; *Top Left*), $App^{f/f}$ (Cre; *Top Right*), $Slc32a1^{CRE}$::FLEX–shCtrl (*Bottom Left*), or $Slc32a1^{CRE}$::FLEX–shAPP (*Bottom Right*) mice. (*G* and *H*) Average mIPSC frequency (*G*) and amplitude (*H*). (*I*) Two-photon time-lapse images of gephyrin puncta and spines on tdTomato and gephyrin intrabody-GFP coexpressing CA1 pyramidal neurons left untreated or treated with 1 μM MDGA1 MAM, treated with 1 μM MDGA1 MAM + 5 μM CGP55845. (*J*) Quantitative analysis of gephyrin puncta elimination rates across conditions at different time points. Filled arrows indicate stable gephyrin clusters, while open arrows show eliminated gephyrin puncta. (*K* and *L*) Average spine density (*K*) and size (*L*) from control and MDGA1 MAM–treated groups. Error bars denote SEM. *P* values determined by Kruskal–Wallis test followed by Dunn's multiple comparison test (*B*, *C*, *G*, and *H*) or two-tailed Student's *t* test (*J*, *K*, and *L*). See Dataset S1 for additional statistics. NS, not significant.

MDGA1 MAM, whereas the interaction of APP with $GABA_BR1a$ was not affected (Fig. 4*D*), implying that MDGA1 MAM at this concentration preferentially binds to MDGA1- or $GABA_BR1a$-unoccupied APP proteins. MDGA2 MAM (1 μM) had no effect on the interaction of APP with MDGA1 or $GABA_BR1a$ (Fig. 4*E*). For technical reasons, we were unable to perform coimmunoprecipitation assays to analyze the interactions of APP with $GABA_BR1$; thus, we employed APP ExD-Fc for pull-down assays. Strikingly, pretreatment with the $GABA_BR$ antagonist CGP55845 (5 μM) failed to prevent the MDGA1 MAM–induced reduction in the mIPSC frequency (*SI Appendix*, Fig. S11 *E–G*). Furthermore, this effect was compromised in hippocampal CA1 neurons innervated by APP-deficient GABAergic interneurons (Fig. 4 *F–H*). However, treatment with MDGA1 MAM significantly reduced the mIPSC frequency in Nlgn2-deficient hippocampal CA1 neurons (*SI Appendix*, Fig. S11 *H–J*), suggesting that MDGA1 MAM specifically targets APP at GABAergic synapses, likely ruling out potential ceiling effects. We next used dual-color time-lapse two-photon microscopy to assess how MDGA1 MAM influences GABAergic synaptic structures on CA1 pyramidal neurons. Intriguingly, we found that the bath application of MDGA1 MAM (1 μM; < 2 h) significantly increased the elimination rate of preexisting gephyrin puncta in a $GABA_BR$-independent manner without affecting excitatory synapses (Fig. 4 *I–L*). Moreover, the MDGA1 MAM–mediated elimination of gephyrin puncta was abolished in APP-deficient hippocampal slices (Fig. 4 *I* and *J*). Together, these observations demonstrate that MDGA1 MAM can bind to and inhibit presynaptic APP function, resulting in impaired GABAergic synaptic transmission in the hippocampal CA1 region.

MDGA1 MAM Impairs Novel Object Recognition. Previous studies showed that the perturbation of APP (and/or APLPs) induces severe cognitive deficits in mice (42, 43). Specifically, forebrain GABAergic neuron-specific APP/APLP2 double-cKO mice exhibit impaired hippocampus-dependent spatial learning and memory (42). Hence, we tested whether MDGA1-induced inhibition of APP function and/or accelerated GABAergic synapse elimination in hippocampal CA1 neurons impacts mouse behavior (Fig. 5). We stereotactically expressed MDGA1 WT, MDGA1 MAM, or ΔMAM in the hippocampal CA1 region of adult mice and performed a battery of behavioral tests 4 wk after injections (Fig. 5 *A* and *B*). Both MDGA1 WT– and ΔMAM-expressing mice exhibited comparable anxiety/exploration-related behavior, working memory, object-location memory, and contextual fear memory (*SI Appendix*, Fig. S12). However, in the novel object-recognition test, in which mice were exposed to two identical objects on the first day (training) and given a new object that replaced one of the two familiar objects on the second day (testing), the discrimination index decreased in MDGA1 WT– or MAM– expressing mice compared with control or MDGA1 ΔMAM– expressing mice (Fig. 5 *C–F*). These results underscore the significance of MDGA1 MAM in compromising object-recognition memory.

Discussion

APP has been a keen focus in the Alzheimer's research fields. Despite extensive studies for more than three decades, the physiological significance of APP remains enigmatic. Our study showed that APP primarily functions at presynaptic neurons in mediating synaptic inhibition in the hippocampal CA1 region. Surprisingly, the loss of APP did not affect glutamatergic synaptic transmission or spine density, implying possible redundancy with other closely related APP homologs (22, 44, 45). However, the deletion of APP, but not APLP2, in hippocampal GABAergic interneurons decreased GABAergic synaptic inputs, suggesting that APP might perform a unique/nonoverlapping physiological role in regulating specific neural circuit properties (see also ref. 42). Our results showed that both cellular and synaptic functions of APP control GABAergic synapse development. APP KD in GABAergic interneurons reduced intrinsic excitability and release probability, resulting in lower GABA release and thereby decreasing the inhibitory synapse density and strength. This impaired inhibitory synaptic function was rescued by the overexpression of both WT APP and ExD-deleted APP. These results show a cellular role for APP in controlling GABAergic synapse development and further suggest that the inhibitory

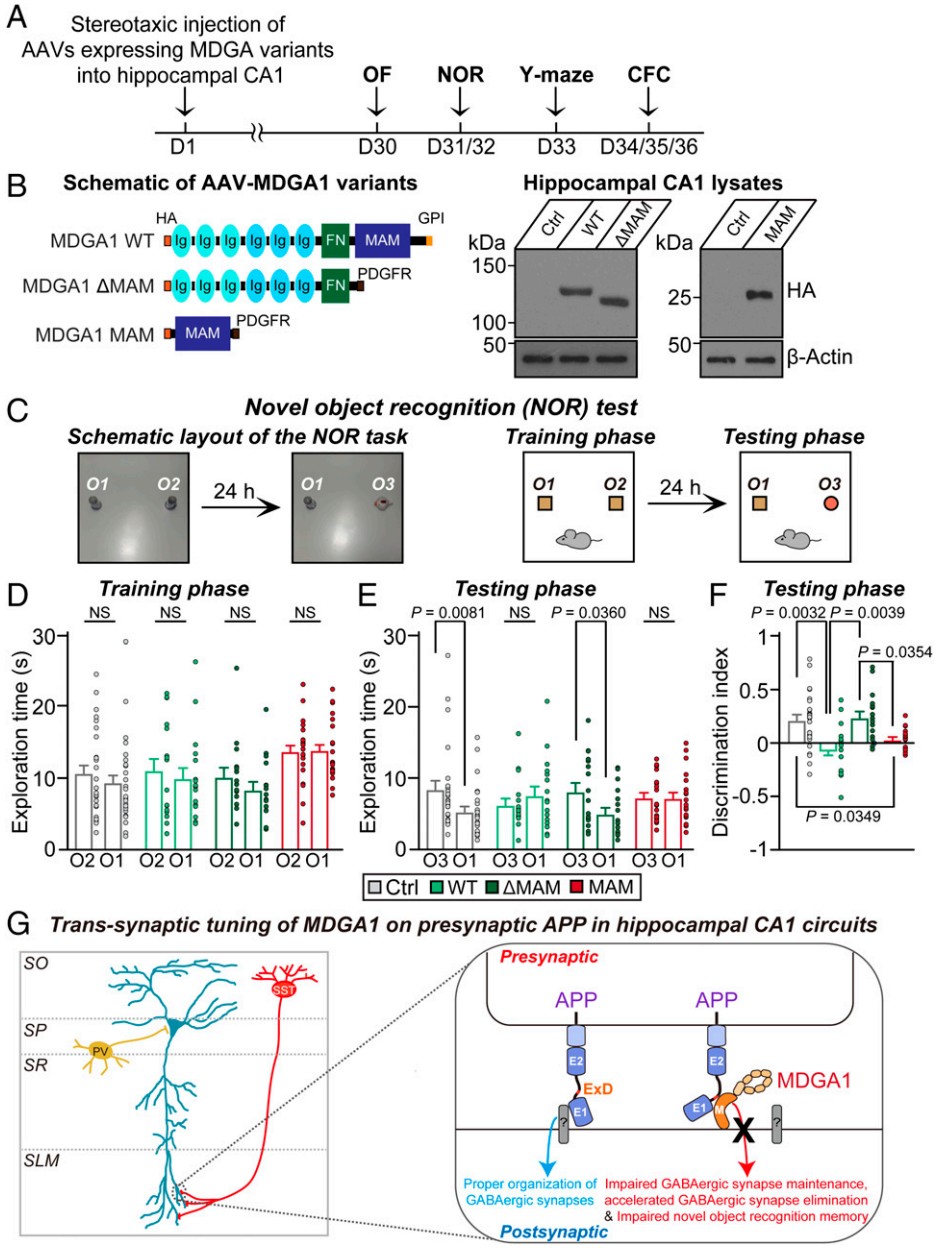

Fig. 5. MDGA1 MAM impairs novel object-recognition memory. (*A*) Schematic diagram of mouse behavioral analyses. The CA1 region of the hippocampus of ~6-wk-old mice was bilaterally injected with AAVs expressing the indicated MDGA1 variants. Injected mice were subjected to various behavioral tasks 4 wk after the injections. CFC, contextual fear conditioning; NOR, novel object-recognition test; OF, open-field test. (*B*) Expression of AAV–MDGA1 variants in the hippocampal CA1 region of injected mice. (*C–F*) Novel object-recognition test. Design of experiments measuring novel object-recognition memories in injected mice (*C*). Two identical objects (O1 and O2) were used for the training phase, and one familiar object (O1) and one novel object (O3) were used for the testing phase. Exploration time (*D* and *E*) and discrimination index (*F*) were measured. (*G*) Model showing how postsynaptic MDGA1 *trans*-synaptically tunes presynaptic APP, which is required for GABAergic synapse stabilization. Error bars denote SEM. *P* values determined by nonparametric Mann–Whitney *U* test (*D* and *E*) or one-way ANOVA with Bonferroni post hoc test (*F*). See Dataset S1 for additional statistics. NS, not significant.

synaptic alterations are likely mediated by reduced activity-dependent synaptogenesis, as local GABA release drives the formation of inhibitory synapses (36). However, our data strongly suggest that the effect of APP on postsynaptic inhibitory synapses is not simply mediated by regulating intrinsic excitability of GABAergic interneurons, which could be controlled by other APP-binding proteins (22, 44, 45). We previously demonstrated that the local GABA release on dendrites is both sufficient and necessary for inhibitory and excitatory synaptogenesis (36), yet we found that the structure and function of excitatory synapses are intact in APP-deficient hippocampal CA1 slices. Strikingly, our study revealed an unanticipated mechanism by which presynaptic APP *trans*-synaptically regulates the postsynaptic properties of GABAergic synapses, showing that postsynaptic MDGA1 likely tunes the *trans*-synaptic function of presynaptic APP. This is evidenced by the absence of a change in mIPSC frequency in MDGA1 ΔMAM–expressing neurons and by the reduced gephyrin elimination rate following MDGA1 MAM treatment in APP-deficient slices. Together, our data show that MDGA1 tunes APP-mediated synaptic inhibition by facilitating the elimination of inhibitory synapses via a *trans*-synaptic action of presynaptic APP. Intriguingly, we found that MDGA1 protein levels were down-regulated in the hippocampus and cerebellar cortex of adult mice subjected to rotarod exercise (*SI Appendix*, Fig. S13). These observations suggest the possibility that the MDGA1–APP complex can be finely tuned in vivo in response to changes in network activities, in line with the previous finding that MDGA1 transcripts are up-regulated upon chronic synaptic activity blockade (46) and in the human–mouse chimeric model of AD (47).

Among the dozens of known APP-binding proteins, $GABA_BR1a$ is responsible for APP-mediated inhibition of glutamate release from excitatory presynaptic terminals (26), a process that likely contributes to the dampening of excessive network activity (48, 49). We found that MDGA1 MAM–driven regulatory mechanisms that act on APP at GABAergic presynaptic terminals are mediated by the $GABA_BR1a$-binding ExD of APP but do so in a $GABA_BR1$-independent manner. This identifies MDGA1 as a "tuner" of APP functions in GABAergic synaptic transmission and suggests that it does not compete with $GABA_BR1a$, which is primarily expressed at presynaptic neurons, where it inhibits glutamate release (50). Although more work is required, we propose that APP might modulate synaptic inhibition in the hippocampal CA1 via two independent pathways: 1) $GABA_BR$-dependent inhibition involving $GABA_BR1a$ and 2) $GABA_BR$-independent disinhibition involving MDGA1. These data suggest that APP might orchestrate specific synaptic/circuit properties in a context-dependent manner by utilizing intrinsically disordered regions to undergo distinct extracellular phase separation (51, 52). Taken together, our data suggest a model in which postsynaptic MDGA1 exerts a profound destabilizing influence on GABAergic synapses and reduces postsynaptic $GABA_AR$-mediated responses, likely by binding to presynaptic APP (Fig. 5*G*). This model posits a unique *trans*-synaptic action of APP distinct from that of other presynaptic adhesion molecules (e.g., Nrxns or Protein tyrosine phosphatase-σ) in controlling different postsynaptic receptor responses (53). It remains to be determined which postsynaptic proteins directly transduce the *trans*-synaptic signals produced by presynaptic APP. Although the *cis*- and/or *trans*-dimerization of APP via the E1 domain facilitates synaptic adhesion (22, 44, 45), whether APP-mediated *trans*-synaptic functions involve an identical mechanism remains to be determined.

A number of our findings obtained using conditional *Mdga1*-KO mice are in stark contrast to prior results obtained using either MDGA-KD approaches or constitutive *Mdga1*-KO mice (16, 17, 21) as follows: 1) postnatal deletion of postsynaptic MDGA1 in hippocampal CA1 neurons does not alter basal GABAergic synaptic transmission; 2) MDGA1 overexpression decreases GABAergic synaptic transmission and density at the dendritic, but not somatic, compartment of hippocampal CA1 neurons; and 3) MDGA1 targets APP, but not Nlgn2, at least at hippocampal CA1 GABAergic neural circuits. However, it is equally plausible that MDGA1 is involved in negative regulation of Nlgn2-mediated somatic inhibition during the early stages of GABAergic synapses in the hippocampus and/or other synapse types. These apparently puzzling observations may be reconciled by positing that MDGA1 acts as a factor that modulates specific context- and activity-dependent feedback inhibition rather than as a mandatory factor for GABAergic synapse formation per se. Future studies are warranted to address a number of important unresolved questions raised by the current study. For example, it remains to be determined whether MDGA1 interacts with both soluble and membrane-anchored APP protein species and if MDGA1 can influence APP proteolytic processing in vivo. Moreover, how APP differentially regulates excitability in GABAergic interneurons compared with excitatory neurons (54) should be scrutinized. Importantly, a better understanding of the MDGA1-mediated dismantling of GABAergic synapses across different neural circuits requires knowing when and how the up-regulation of MDGA1 is achieved.

Given the strong association of APP with AD and MDGA1 with late-onset AD (23, 55), it is plausible that dysfunctions in the MDGA1–APP complex are linked to AD pathogenesis. However, accumulating evidence also points to a possible association of APP with autism spectrum disorders or schizophrenia (56–58) and the association of MDGA1 with schizophrenia (59). Future studies should systematically examine how the dysregulation of the MDGA1–APP complex elicits different manifestations during postnatal development.

APP ExD was recently proposed as a potential therapeutic agent for related neuropsychiatric disorders associated with the $GABA_BR$ complex (26, 39, 60, 61). However, given the promiscuous nature of the APP ExD, which binds to $GABA_BR1a$, MDGA1, and possibly other unidentified ligands, alternative therapeutic strategies for modulating specific APP interactome(s) should be considered. The determination of the structure of the MDGA1–APP complex will pave the way for future efforts to modulate the multiple APP ExD-mediated interactions and control intrinsic neuronal excitability at specific GABAergic neural circuits.

Materials and Methods

Animals, expression vectors, and antibodies are described in *SI Appendix, SI Materials and Methods*. Also see *SI Appendix, SI Materials and Methods* for details of the generation of *Mdga2* conditional mice, affinity chromatography, in-gel digestion and liquid chromatography–MS/MS analysis, production of recombinant Ig fusion proteins from HEK293T cells, cell-surface–binding assays, pull-down assays, coimmunoprecipitation assays, qRT-PCR, expression and purification of APP and MDGA1 proteins for biophysics experiments, small-angle X-ray scattering, biophysical characterization, affinity measurement using a cell-based enzyme-linked immunosorbent assay, preparation of cultured hippocampal neurons, virus generation, stereotaxic surgery and virus injection, immunocytochemistry, organotypic slice preparation and transfection, viral infections of organotypic hippocampal slice cultures, two-photon imaging, quantification of dendritic spines, quantification of gephyrin puncta, electrophysiology, behavioral analyses, and statistical analyses.

Data Availability. All study data are included in the article and/or supporting information.

ACKNOWLEDGMENTS. We are grateful to Jinha Kim (Daegu Gyeongbuk Institute of Science and Technology [DGIST]) for technical assistance, Dr. Thomas Südhof (Stanford University) for the gift of Nlgn2 floxed mice, Dr. Dennis O'Leary (Salk Institute) for the gift of MDGA1 floxed mice, Dr. Joris de Wit (Katholieke Universiteit Leuven) for the gift of $GABA_BR$ constructs, Dr. Bart de Strooper (University College London) for the gift of APP antibody, Dr. Eunjoon Kim (Korea Advanced Institute of Science and Technology/Institute for Basic Science) for the gift of Cre-driver lines, and

Dr. Wookyung Yu (DGIST) for advice on biophysics experiments. This work was supported by grants from the Brain Research Program through the NRF funded by the Ministry of Science, Information and Communication Technology, and Future Planning (2017M3C7A1023470 and 2021R1A2C1091863 to J. Ko), the Future Planning (2019R1A2C108604 to J.W.U.), the DGIST R & D Program of the Ministry of Science and ICT (21-CoE-BT-01 to J.W.U. and J. Ko), the NIH (R01MH124778 and R21MH126073 to W.C.O. and T32NS099042 to R.O.), the Brain and Behavioral Research Foundation NARSAD Young Investigator Award (to W.C.O.), the Brain Research Foundation Seed Grant (to W.C.O.), Colorado State University/University of Colorado-Pilot Collaboration Award (to W.C.O.), Jane and Aatos Erkko Foundation (to T.K.), and a KBSI grant (C060100 to J.Y.K.).

1. A. E. West, Activity-dependent transcription collaborates with local dendritic translation to encode stimulus-specificity in the genome binding of NPAS4. *Neuron* **104**, 634–636 (2019).
2. E. H. Buhl *et al.*, Physiological properties of anatomically identified axo-axonic cells in the rat hippocampus. *J. Neurophysiol.* **71**, 1289–1307 (1994).
3. T. W. Blackstad, P. R. Flood, Ultrastructure of hippocampal axo-somatic synapses. *Nature* **198**, 542–543 (1963).
4. N. A. Lambert, W. A. Wilson, Heterogeneity in presynaptic regulation of GABA release from hippocampal inhibitory neurons. *Neuron* **11**, 1057–1067 (1993).
5. T. F. Freund, I. Katona, Perisomatic inhibition. *Neuron* **56**, 33–42 (2007).
6. R. Miles, K. Tóth, A. I. Gulyás, N. Hájos, T. F. Freund, Differences between somatic and dendritic inhibition in the hippocampus. *Neuron* **16**, 815–823 (1996).
7. O. Yizhar *et al.*, Neocortical excitation/inhibition balance in information processing and social dysfunction. *Nature* **477**, 171–178 (2011).
8. S. B. Nelson, V. Valakh, Excitatory/inhibitory balance and circuit homeostasis in autism spectrum disorders. *Neuron* **87**, 684–698 (2015).
9. T. C. Südhof, Synaptic neurexin complexes: A molecular code for the logic of neural circuits. *Cell* **171**, 745–769 (2017).
10. A. Poulopoulos *et al.*, Neuroligin 2 drives postsynaptic assembly at perisomatic inhibitory synapses through gephyrin and collybistin. *Neuron* **63**, 628–642 (2009).
11. J. R. Gibson, K. M. Huber, T. C. Südhof, Neuroligin-2 deletion selectively decreases inhibitory synaptic transmission originating from fast-spiking but not from somatostatin-positive interneurons. *J. Neurosci.* **29**, 13883–13897 (2009).
12. H. Ali, L. Marth, D. Krueger-Burg, Neuroligin-2 as a central organizer of inhibitory synapses in health and disease. *Sci. Signal.* **13**, eabd8379 (2020).
13. S. A. Connor, J. Elegheert, Y. Xie, A. M. Craig, Pumping the brakes: Suppression of synapse development by MDGA-neuroligin interactions. *Curr. Opin. Neurobiol.* **57**, 71–80 (2019).
14. J. W. Um, J. Ko, Neural glycosylphosphatidylinositol-anchored proteins in synaptic specification. *Trends Cell Biol.* **27**, 931–945 (2017).
15. A. Takeuchi, D. D. O'Leary, Radial migration of superficial layer cortical neurons controlled by novel Ig cell adhesion molecule MDGA1. *J. Neurosci.* **26**, 4460–4464 (2006).
16. K. Lee *et al.*, MDGAs interact selectively with neuroligin-2 but not other neuroligins to regulate inhibitory synapse development. *Proc. Natl. Acad. Sci. U.S.A.* **110**, 336–341 (2013).
17. K. L. Pettem, D. Yokomaku, H. Takahashi, Y. Ge, A. M. Craig, Interaction between autism-linked MDGAs and neuroligins suppresses inhibitory synapse development. *J. Cell Biol.* **200**, 321–336 (2013).
18. J. A. Kim *et al.*, Structural insights into modulation of neurexin-neuroligin trans-synaptic adhesion by MDGA1/neuroligin-2 complex. *Neuron* **94**, 1121–1131 (2017).
19. S. P. Gangwar *et al.*, Molecular mechanism of MDGA1: Regulation of neuroligin 2:neurexin trans-synaptic bridges. *Neuron* **94**, 1132–1141 (2017).
20. J. Elegheert *et al.*, Structural mechanism for modulation of synaptic neuroligin-neurexin signaling by MDGA proteins. *Neuron* **95**, 896–913 (2017).
21. S. A. Connor *et al.*, Loss of synapse repressor MDGA1 enhances perisomatic inhibition, confers resistance to network excitation, and impairs cognitive function. *Cell Rep.* **21**, 3637–3645 (2017).
22. U. C. Müller, T. Deller, M. Korte, Not just amyloid: Physiological functions of the amyloid precursor protein family. *Nat. Rev. Neurosci.* **18**, 281–298 (2017).
23. D. J. Selkoe, J. Hardy, The amyloid hypothesis of Alzheimer's disease at 25 years. *EMBO Mol. Med.* **8**, 595–608 (2016).
24. X. Zhang *et al.*, An APP ectodomain mutation outside of the Aβ domain promotes Aβ production in vitro and deposition in vivo. *J. Exp. Med.* **218**, e20210313 (2021).
25. M. C. Dinamarca *et al.*, Complex formation of APP with $GABA_B$ receptors links axonal trafficking to amyloidogenic processing. *Nat. Commun.* **10**, 1331 (2019).
26. H. C. Rice *et al.*, Secreted amyloid-β precursor protein functions as a $GABA_B$R1a ligand to modulate synaptic transmission. *Science* **363**, eaao4827 (2019).
27. I. Coburger *et al.*, Analysis of the overall structure of the multi-domain amyloid precursor protein (APP). *PLoS One* **8**, e81926 (2013).
28. P. Marchand, M. Volkmann, J. S. Bond, Cysteine mutations in the MAM domain result in monomeric meprin and alter stability and activity of the proteinase. *J. Biol. Chem.* **271**, 24236–24241 (1996).
29. V. B. Cismasiu, S. A. Denes, H. Reiländer, H. Michel, S. E. Szedlacsek, The MAM (meprin/A5-protein/PTPmu) domain is a homophilic binding site promoting the lateral dimerization of receptor-like protein-tyrosine phosphatase mu. *J. Biol. Chem.* **279**, 26922–26931 (2004).
30. H. Chen, Z. He, A. Bagri, M. Tessier-Lavigne, Semaphorin-neuropilin interactions underlying sympathetic axon responses to class III semaphorins. *Neuron* **21**, 1283–1290 (1998).
31. F. Nakamura, M. Tanaka, T. Takahashi, R. G. Kalb, S. M. Strittmatter, Neuropilin-1 extracellular domains mediate semaphorin D/III-induced growth cone collapse. *Neuron* **21**, 1093–1100 (1998).
32. T. Yelland, S. Djordjevic, Crystal structure of the neuropilin-1 MAM domain: Completing the neuropilin-1 ectodomain picture. *Structure* **24**, 2008–2015 (2016).
33. J. Rudan Njavro *et al.*, Mouse brain proteomics establishes MDGA1 and CACHD1 as in vivo substrates of the Alzheimer protease BACE1. *FASEB J.* **34**, 2465–2482 (2020).
34. K. A. Pelkey *et al.*, Hippocampal GABAergic inhibitory interneurons. *Physiol. Rev.* **97**, 1619–1747 (2017).
35. K. H. Loh *et al.*, Proteomic analysis of unbounded cellular compartments: Synaptic clefts. *Cell* **166**, 1295–1307 (2016).
36. W. C. Oh, S. Lutzu, P. E. Castillo, H. B. Kwon, De novo synaptogenesis induced by GABA in the developing mouse cortex. *Science* **353**, 1037–1040 (2016).
37. M. Hick *et al.*, Acute function of secreted amyloid precursor protein fragment APPsα in synaptic plasticity. *Acta Neuropathol.* **129**, 21–37 (2015).
38. B. Wang *et al.*, The amyloid precursor protein controls adult hippocampal neurogenesis through GABAergic interneurons. *J. Neurosci.* **34**, 13314–13325 (2014).
39. H. C. Rice *et al.*, Contribution of GABAergic interneurons to amyloid-β plaque pathology in an APP knock-in mouse model. *Mol. Neurodegener.* **15**, 3 (2020).
40. B. L. Tang, Amyloid precursor protein (APP) and GABAergic neurotransmission. *Cells* **8**, 550 (2019).
41. M. Chen *et al.*, APP modulates KCC2 expression and function in hippocampal GABAergic inhibition. *eLife* **6**, e20142 (2017).
42. A. Mehr *et al.*, Lack of APP and APLP2 in GABAergic forebrain neurons impairs synaptic plasticity and cognition. *Cereb. Cortex* **30**, 4044–4063 (2020).
43. V. Steubler *et al.*, Loss of all three APP family members during development impairs synaptic function and plasticity, disrupts learning, and causes an autism-like phenotype. *EMBO J.* **40**, e107471 (2021).
44. M. Nicolas, B. A. Hassan, Amyloid precursor protein and neural development. *Development* **141**, 2543–2548 (2014).
45. U. C. Müller, H. Zheng, Physiological functions of APP family proteins. *Cold Spring Harb. Perspect. Med.* **2**, a006288 (2012).
46. M. M. Silva *et al.*, MicroRNA-186-5p controls GluA2 surface expression and synaptic scaling in hippocampal neurons. *Proc. Natl. Acad. Sci. U.S.A.* **116**, 5727–5736 (2019).
47. I. Espuny-Camacho *et al.*, Hallmarks of Alzheimer's disease in stem-cell-derived human neurons transplanted into mouse brain. *Neuron* **93**, 1066–1081 (2017).
48. P. Tosetti, N. Ferrand, I. Colin-Le Brun, J. L. Gaïarsa, Epileptiform activity triggers long-term plasticity of GABA(B) receptor signalling in the developing rat hippocampus. *J. Physiol.* **568**, 951–966 (2005).
49. F. M. Werner, R. Coveñas, Neural networks in generalized epilepsy and novel antiepileptic drugs. *Curr. Pharm. Des.* **25**, 396–400 (2019).
50. R. Vigot *et al.*, Differential compartmentalization and distinct functions of GABAB receptor variants. *Neuron* **50**, 589–601 (2006).
51. D. Snead, D. Eliezer, Intrinsically disordered proteins in synaptic vesicle trafficking and release. *J. Biol. Chem.* **294**, 3325–3342 (2019).
52. Z. Feng, X. Chen, X. Wu, M. Zhang, Formation of biological condensates via phase separation: Characteristics, analytical methods, and physiological implications. *J. Biol. Chem.* **294**, 14823–14835 (2019).
53. H. Y. Kim, J. W. Um, J. Ko, Proper synaptic adhesion signaling in the control of neural circuit architecture and brain function. *Prog. Neurobiol.* **200**, 101983 (2021).
54. S. H. Lee *et al.*, APP family regulates neuronal excitability and synaptic plasticity but not neuronal survival. *Neuron* **108**, 676–690.e8 (2020).
55. B. Zhang *et al.*, Integrated systems approach identifies genetic nodes and networks in late-onset Alzheimer's disease. *Cell* **153**, 707–720 (2013).
56. A. Alexiou, G. Soursou, N. S. Yarla, G. Md Ashraf, Proteins commonly linked to autism spectrum disorder and Alzheimer's disease. *Curr. Protein Pept. Sci.* **19**, 876–880 (2018).
57. C. J. Westmark *et al.*, APP causes hyperexcitability in fragile X mice. *Front. Mol. Neurosci.* **9**, 147 (2016).
58. E. B. Tereshkina *et al.*, Decrease in 130 kDa- amyloid protein precursor protein (APP) and APP protein ratio in schizophrenia platelets. *Neurosci. Lett.* **725**, 134914 (2020).
59. J. Li *et al.*, The MDGA1 gene confers risk to schizophrenia and bipolar disorder. *Schizophr. Res.* **125**, 194–200 (2011).
60. S. S. Harris, F. Wolf, B. De Strooper, M. A. Busche, Tipping the scales: Peptide-dependent dysregulation of neural circuit dynamics in Alzheimer's disease. *Neuron* **107**, 417–435 (2020).
61. A. Sierksma, V. Escott-Price, B. De Strooper, Translating genetic risk of Alzheimer's disease into mechanistic insight and drug targets. *Science* **370**, 61–66 (2020).